

# High temperature dynamics in quantum compass models

A.K.R. Briffa<sup>1</sup> and X. Zotos<sup>1,2,3,4</sup>

<sup>1</sup>*ITCP and CCQC, Department of Physics, University of Crete, 71003 Heraklion, Greece*

<sup>2</sup>*Foundation for Research and Technology - Hellas, 71110 Heraklion, Greece*

<sup>3</sup>*Max-Planck-Institut für Physik Komplexer Systeme, 01187 Dresden, Germany and*

<sup>4</sup>*Leibniz Institute for Solid State and Materials Research IFW Dresden, 01171 Dresden, Germany*

(Dated: October 4, 2018)

We analyze the high temperature spin dynamics of quantum compass models using a moment expansion. We point out that the evaluation of moments maps to the enumeration of paths in a branching process on the lattice. This mapping to a statistical mechanics combinatorics problem provides an elegant visualization of this analysis. We present results for the time dependent spin correlation function (which is of relevance to NMR experiments) for two compass models: the honeycomb (- Kitaev) and 2D compass model. Furthermore, following this novel approach, we argue that in quantum compass models the spin correlations are generically strongly anisotropic and short ranged.

## INTRODUCTION

Over the years quantum Compass models have proved especially relevant in the modeling of materials with multi-orbital degrees of freedom[1]; these Hamiltonians describe fictitious spin degrees of freedom that have fully anisotropic spatial interactions[2]. Currently they are very prominent in both theoretical and experimental studies of the physics of iridium-oxide materials[3], the  $\alpha$ -RuCl<sub>3</sub> compound[4, 5] and finally the purported application of the Kitaev model[6] to quantum computing. Neutron scattering[7] and NMR experiments[8] have provided convincing evidence that Kitaev model physics dominates the effective Hamiltonian describing  $\alpha$ -RuCl<sub>3</sub>, although the inclusion of further interactions, especially Heisenberg exchange, seem to be necessary for a consistent description of the experiments. Additionally, thermal conductivity experiments could shed more light on the relevant interactions in these exotic quantum magnets.

The canonical theoretical approach to the spin dynamics analysis of the Kitaev model is the elegant and powerful Majorana fermion solution[6]. So far most studies have focused on the zero temperature limit[4, 5]. However, at finite temperatures Monte Carlo methods have been used[9] to sample the auxiliary Majorana fields and there are Exact Diagonalization studies on restricted lattices[10].

In the high temperature limit, a long standing approach to spin dynamics has been the moment method[11]. In this work, we point out that the peculiar structure of compass model Hamiltonians maps the moment enumeration to a branching model, though there are certain extra initial constraints specific to each model. In the following, we discuss as examples the compass model on the two dimensional honeycomb lattice (the so called Kitaev model) and the two-dimensional compass model on a square lattice.

Our main focus is to obtain the salient features of the

exact spin autocorrelation functions from the mapping to model branching processes and compare them to results obtained by diagonalization of the Hamiltonian (ED) on finite size lattices. The validity of the mapping is supported by the agreement with frequency spectra obtained by ED. It is amusing that such simple combinatorial models reproduce the essential features of these quantum many-body models, providing another instance of correspondence between quantum mechanical and statistical mechanics problems. It would be interesting also to consider the inverse procedure, where a classical statistical mechanics problem can be solved by a corresponding quantum compass models.

## METHOD

Primarily we are interested in the evaluation of the spin autocorrelation function

$$C(t) = \langle \tau_0^z(t) \tau_0^z \rangle \quad (1)$$

where  $\tau^\alpha$ ,  $\alpha = x, y, z$  are Pauli spin-1/2 operators, and  $\tau_0^z(t) = e^{+iHt} \tau_0^z e^{-iHt}$ ,  $\hbar = 1$ . We will also briefly discuss further spatial correlations,

$$C_{ij}(t) = \langle \tau_j^z(t) \tau_i^z \rangle, \quad i \neq j. \quad (2)$$

$\langle \dots \rangle$  denotes a thermal average at temperature  $T$  (with  $\beta = 1/T$ ). In the infinite temperature limit,  $\beta \rightarrow 0$ , the autocorrelation function reduces to a trace over all the Hilbert space,

$$C(t) = \frac{1}{2^L} \text{tr} \tau_0^z(t) \tau_0^z \quad (3)$$

$L$  being the number of spins on the lattice.

Expanding in powers of time,

$$C(t) = \sum_{k=0}^{\infty} \frac{(-1)^k}{(2k)!} \mu_{2k} t^{2k} \quad (4)$$

the autocorrelation function analysis reduces to the evaluation of the moments  $\mu_{2k}$ [11],

$$\mu_{2k} = \frac{1}{2L} \text{tr} \tau_0^z \mathcal{L}^{2k} \tau_0^z \quad (5)$$

where  $\mathcal{L} = [H, A] = HA - AH$  is the Liouville operator. The time Fourier transform of  $C(t)$ ,

$$S(\omega) = \int_{-\infty}^{+\infty} C(t) e^{+i\omega t} dt \quad (6)$$

can alternatively be evaluated by an extension in complex frequencies  $z$ ,

$$c(z) = \int_0^{+\infty} C(t) e^{-zt} dt, \quad \Re(z) > 0, \quad (7)$$

$$S(\omega) = \lim_{\eta \rightarrow 0^+} 2\Re[c(\eta - i\omega)]. \quad (8)$$

$c(z)$  is then conveniently expressed as a continued fraction expansion,

$$c(z) = \frac{1}{z + \frac{\Delta_1}{z + \frac{\Delta_2}{z + \dots}}} \quad (9)$$

with the coefficients  $\Delta_n$  related the moments  $\mu_{2k}$  by recursion relations[11].

In the following we will present an approximate evaluation of the moments  $\mu_{2k}$  and the corresponding structure of  $\Delta_n$  by mapping them to combinatorial branching models.

### KITAEV MODEL

The Kitaev model on a honeycomb lattice is given by the Hamiltonian,

$$H = -J_x \sum_{\langle ij \rangle_x} \tau_i^x \tau_j^x - J_y \sum_{\langle ij \rangle_y} \tau_i^y \tau_j^y - J_z \sum_{\langle ij \rangle_z} \tau_i^z \tau_j^z \quad (10)$$

where  $\langle ij \rangle_{x,y,z}$  denotes the nearest neighbor bonds in the three directions on the lattice, with the convention indicated in Fig.1(0). The central operator  $\tau^z$  (that subsequently is abbreviated just by  $\mathbf{z}$ ) represents the operator  $\tau_0^z(t)$  at the initial time  $t = 0$ .

We find that repeatedly applying the Liouville operator  $\mathcal{L}$ , as in (5), creates strings of operators depicted in the subsequent parts of Fig.1. Because of the 3-fold geometry of the honeycomb lattice, the string operators are organized into three branches, each one starting with an  $xx$ ,  $yy$  or  $zz$  bond.

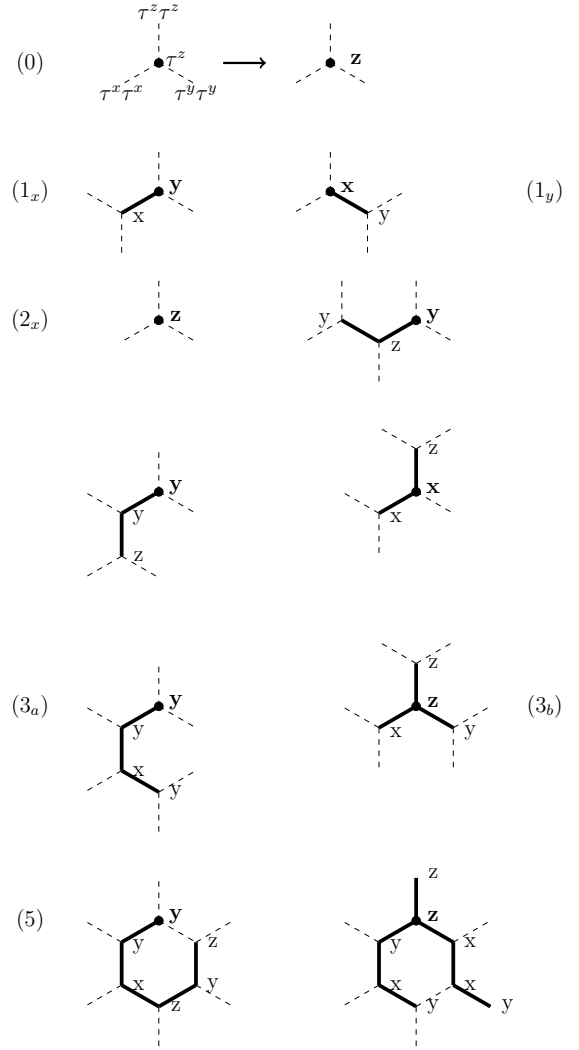


FIG. 1. Indicative branching processes on the Kitaev model on a honeycomb lattice.

Fig.1(1<sub>x</sub>), (1<sub>y</sub>) indicate the two possible operator strings created by one application of  $\mathcal{L}$  on  $\tau_0^z(t = 0)$ . The third sting, along the  $z$ -bond, vanishes at this order. In (2<sub>x</sub>) the four possible (non-vanishing) strings created by the application of  $\mathcal{L}$  on (1<sub>x</sub>) are shown (note that there are an additional four, symmetrically related, strings for (1<sub>y</sub>) which are not shown). Then, the application of the trace in (5) gives zero for all but the first diagram shown in Fig.1(2<sub>x</sub>): the zero-length string which is just the operator  $\tau_0^z$ . Consequently there are only two contributions to the second moment,  $\mu_2$ : this one and the analogous diagram arising from the application of  $\mathcal{L}$  on (1<sub>y</sub>). The problem of applying  $\mathcal{L}$  on a operator string is therefore mapped to a branching process in three directions, where at each iteration the tail operator in a branch either dis-

appears or a new one is created in one of the three possible directions (although with some specific restrictions at the origin which we will discuss later).

In the high temperature limit, the trace of any string of non-zero length vanishes. Thus, evaluating the moments reduces to counting all of the possible branching processes that culminate in the complete annihilation of the strings (i.e. they return to just a single  $\tau_0^z$  operator). Each branching configuration contributes a factor of  $(\pm 2iJ_\alpha)$  from each application of  $\mathcal{L}$  to the value of the contribution to a moment. This arises from the spin commutation involving the bond- $\alpha$ ; the factor for annihilating a particular link turns out to always have the opposite sign to that corresponding to its creation. As an example, the third order diagram shown in Fig.1(3a) represents the operator string:  $(-2iJ_y)(-2iJ_z)(+2iJ_x)\tau_3^y\tau_2^x\tau_1^y\tau_0^y$ . Henceforth we will only consider  $J_x = J_y = J_z$ , although generalising to the anisotropic case is more complex but feasible. In summary, it therefore seems that the minimal model is branching in three independent directions. However, as we will now discuss, this is not quite adequate. There are some extra initial constraints and also some "higher order" processes that need consideration.

We find that the branching model obeys the following rules:

- (i) side-branching is not possible and the operator at a vertex is given by the direction of the missing bond;
- (ii) applying  $\mathcal{L}$  in the middle of a branch annihilates the entire operator string;
- (iii) independent branching along all three directions is not possible: there are initial restrictions. A branch along the  $z$ -direction cannot be created at first order. Instead, it can only be initiated when either an  $x$ -direction or a  $y$ -direction branch already exists, as depicted in Fig.1(2 $_x$ ). This initial restriction effects the lowest order moments and thus the high frequency behavior of the spectral function.
- (iv) Branches must be annihilated in the reverse order to which they were created or the contribution from the entire string vanishes.
- (v) Possible higher order processes are not taken into account where the branching structure is modified e.g. at the origin and then eventually reconstructed and annihilated.
- (vi) Finally, as shown in Fig.1(5), the branching process is self-avoiding.

In the inset of Fig.1 we show the values of  $\Delta_n$  evaluated from the moments  $\mu_{2k}$  for the two models, the branching process without (shown in red) and with (shown in black) the initial constraints. It is clear that for large values of  $n$  the  $\Delta_n$ 's asymptotically coincide. In these branching model calculations, however, we have omitted the self-avoidance constraint.

To estimate the applicability of the branching model we compare in Fig.1 the spectra obtained by the branching models with (C) and without (UN) initial constraints.

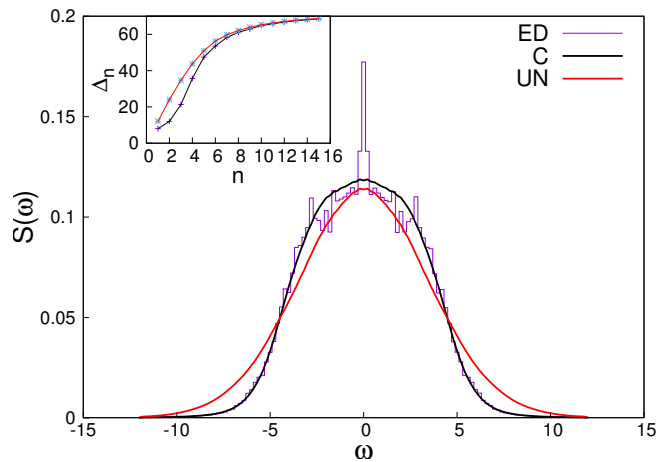


FIG. 2. Spectrum of Kitaev model, by ED, branching model without (UN) and with (C) initial constraints; inset: corresponding  $\Delta_n$  values.

Also shown are results from an exact diagonalization study (ED) on a lattice of 4 by 6 spins. with periodic boundary conditions. Here we calculated in the high temperature limit using the microcanonical Lanczos method[13]. 100 Lanczos iterations were used to converge to an infinite temperature state and 400 further iterations to obtain the continuous fraction expansion. The  $\delta$ -function peak at zero frequency is a finite size effect due to an excess of degenerate states in small lattices. The agreement is fair with the model when including initial constraints (despite omitting the self-avoidance requirement) and can be fitted by a form  $S_{fit}(\omega) \sim a/(b + \omega^6)$ . We should stress that this frequency dependence is way off a Gaussian or Lorentzian form.

## 2D COMPASS MODEL

Next, we will study the 2D-compass model, using the same approach as previously. The Hamiltonian is given by,

$$H = -J_x \sum_{\langle ij \rangle_x} \tau_i^x \tau_j^x - J_y \sum_{\langle ij \rangle_y} \tau_i^y \tau_j^y \quad (11)$$

with the bond-labeling convention used depicted in Fig.3(0).

Analogously to our discussion of the Kitaev model, repeated applications of the Liouville operator creates strings of operators which can propagate with up to four branches: see Fig.3. The same procedure for obtaining the moments  $\mu_{2k}$  and corresponding  $\Delta_n$  of this combinatorial model can then be applied, but with the same reservations on possibly omitted high-order processes.

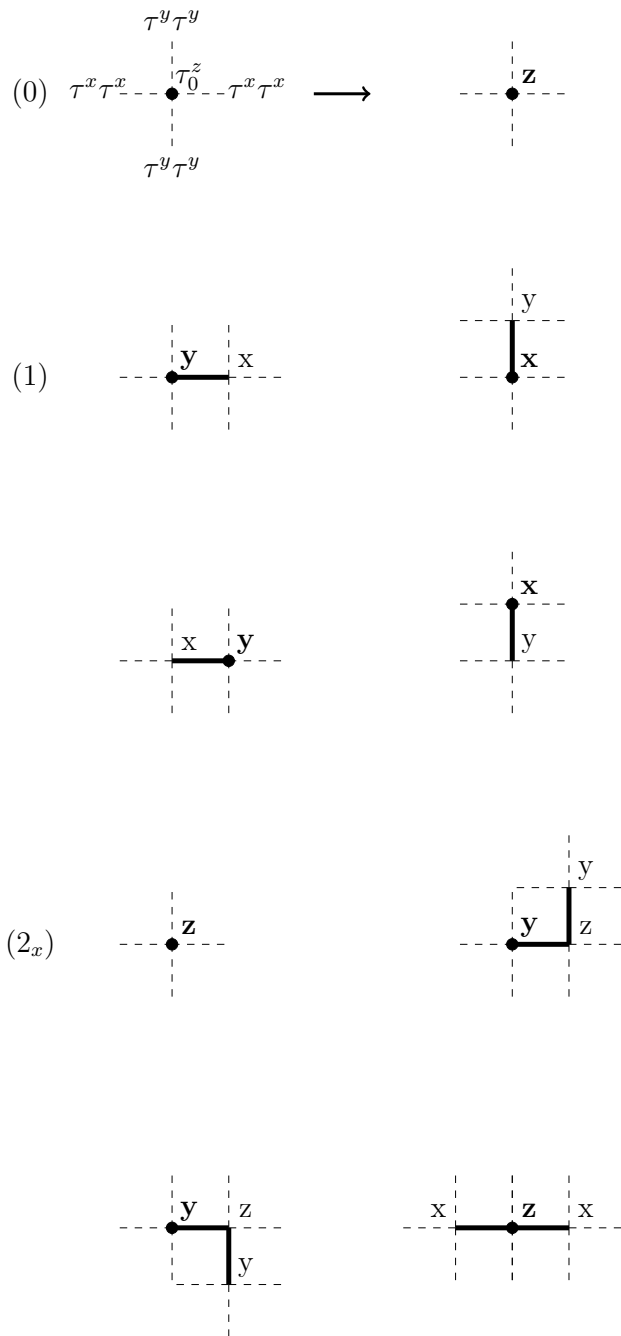


FIG. 3. Indicative branching processes for the 2D compass model on a square lattice.

This time there are a different set of restrictions specific to the 2D compass model. Firstly, we find that the operator strings must propagate alternatively along  $x$ -links and  $y$ -links. Trying to extend the string along two consecutive  $x$ -links (or  $y$ -links) causes the entire string to vanish. This also means that the internal spin operators along the length of the string are all  $\tau^z$ 's. Secondly, we

note that, as there was in the Kitaev model, there are initial constraints on the order in which the four different branches can be created and subsequently destroyed. Finally, the branching model is again self-avoiding.

To investigate the infinite temperature spin-autocorrelation for the isotropic 2D compass model we have calculated a finite number of moments for two different branching models: one which includes the initial constraints, and one with out. In both cases, however, we have again omitted the self-avoidance requirement. The  $\Delta_n$  parameters that we have calculated are shown in the inset of Fig.4.

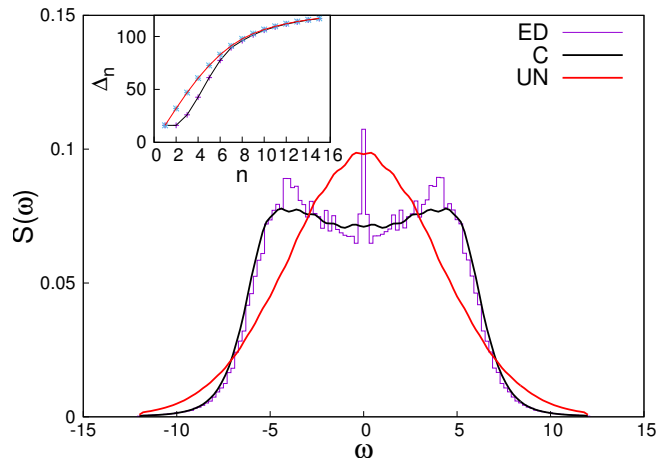


FIG. 4. Spectrum of the 2D compass model by ED, branching model without (UN) and with (C) initial constraints; inset: corresponding  $\Delta_n$  values.

The subsequent  $S(\omega)$  spectrum is shown in Fig.4 for the branching model including the initial branch-creation-order constraint (C) and without this initial constraint (UN). These are compared to the spectrum obtained by a microcanonical Lanczos calculation (ED) on a lattice of 4 by 6 spins. It is interesting to see that even the non-monotonic behaviour of  $S(\omega)$  is reproduced when including the initial branch-creation-order constraint. In contrast, the unconstrained branching behaviour cannot capture this, indicating that it arises due to the degeneracy of the first two  $\Delta$  values.

By using the same approach of expanding the time dependance as a function of the Liouville operator, we can also consider further-range spin correlation in the high temperature limit.

$$C_{0j}(t) = \frac{1}{2L} \text{tr} \tau_j^\alpha(t) \tau_0^\alpha. \quad (12)$$

Consequently, we deduce, that for  $j \neq 0$  all correlations vanish in the infinite temperature limit. This occurs because the initial pair of operators  $\tau_j^\alpha \tau_0^\alpha$  cannot be reduced to the identity by application of  $\mathcal{L}$ . We can also consider finite temperatures by expanding  $e^{-\beta H}$  in powers

of  $H$ . Then we can plausibly argue that we obtain a finite value for the correlations  $\langle \tau_j^\alpha(t) \tau_0^\alpha \rangle$ , only when  $j$  is a nearest neighbor site in the  $\alpha$ - lattice direction. However, further-neighbour correlations all vanish identically at all temperatures. Again, this is because it is impossible to reduce any of the resulting operator strings to the identity by application of either  $\mathcal{L}$  or  $H$ . This result has already been found for the Kitaev model using the Majorana fermion approach[12]. Following the same line of reasoning, in the 2D compass model the  $\tau_j^\alpha \tau_0^\alpha$  correlations are nonzero only at finite temperatures and only when the spins  $\tau_0^\alpha$ ,  $\tau_j^\alpha$  are on the same  $\alpha$ - direction chain. Similar considerations also apply to higher dimensionality quantum compass models.

In conclusion, the above analysis, to an extent heuristic, provides an interesting novel perspective. Firstly, we have discovered that the high temperature spin-autocorrelation function of quantum compass models can be mapped onto a statistical-mechanical branching problem (along with some additional, model-specific restrictions). We have discussed the results from calculating a finite number of moments for two different isotropic compass models, investigating the effects of appropriately including the model-specific initial restricts on the branching-scheme. Despite omitting the self-avoidance requirement, this provided a useful insight into the shape of these correlation functions. These techniques also have the potential to be generalised to anisotropic couplings  $J_x \neq J_y \neq J_z$  and the evaluation of finite temperature correlations. It may be feasible to obtain analytic expressions for the moments of a constraint-free branching model, but it is clear that an exact evaluation of the autocorrelation function requires the implementation of self-avoidance, which is well-known to be a highly non-trivial problem. This raises the interesting perspective of whether the inverse procedure could be used to solve self-avoiding statistical mechanics problems by means of a mapping onto a corresponding quantum compass model. It appears to be another instance of correspondence between quantum mechanical and statistical mechanics problems. Finally, we note that other types of correlations functions, for example those related to trans-

port properties, can also be studied using this technique.

## ACKNOWLEDGMENTS

This work was supported by the European Union Program No. FP7-REGPOT-2012-2013-1 under Grant No. 316165. A.K.R.B. acknowledges the hospitality of MPI - PKS extended to her during visits. X.Z. acknowledges fruitful discussions with B. Büchner, C. Hess, S. Miyashita, H. Tsunetsugu, the hospitality of the Institute for Solid State Physics - U. Tokyo and support by the Alexander von Humboldt Foundation.

- 
- [1] K. Kugel, and D. Khomskii, *Sov. Phys. Usp.* **25**, 231 (1982).
  - [2] Z. Nussinov and J. van den Brink, *Rev. Mod. Phys.* **87**, 1 (2015).
  - [3] G. Jackeli, G. Khaliullin, *Phys. Rev. Lett.* **102**, 017205 (2009).
  - [4] J. Knolle, D. L. Kovrizhin, J. T. Chalker, and R. Moessner, *Phys. Rev. Lett.* **112**, 207203 (2014); *Phys. Rev. B* **92**, 115127 (2015).
  - [5] F. Zschocke and M. Vojta, *Phys.Rev. B* **92**, 014403 (2015).
  - [6] A. Yu. Kitaev, *Ann. Phys. (Amsterdam)* **321**, 2 (2006).
  - [7] A. Banerjee, C.A. Bridges, J-Q. Yan, A.A. Aczel, L. Li, M.B. Stone, G.E. Granroth, M.D. Lumsden, Y. Yiu, J. Knolle, D.L. Kovrizhin, S. Bhattacharjee, R. Moessner, D.A. Tennant, D.G. Mandrus, S.E. Nagler, *Nature Materials* **15**, 733 (2016)
  - [8] S.-H. Baek, S.-H. Do, K.-Y. Choi, Y.S. Kwon, A.U.B. Wolter, S. Nishimoto, Jeroen van der Brink, and B. Büchner, arXiv: 1702.01671
  - [9] J. Nasu, M. Udagawa and Y. Motome, *Phys.Rev. B* **92**, 115122 (2015).
  - [10] A. Metavitsiadis and W. Brenig, arXiv:1605.09390.
  - [11] M. Böhm, V.S. Viswanath, J. Stolze and G. Müller, *Phys.Rev. B* **49**, 15669 (1994).
  - [12] G. Baskaran, Saptarshi Mandal, and R. Shankar, *Phys. Rev. Lett.* **98**, 247201 (2007).
  - [13] M. W. Long, P. Prelovsek, S. El Shawish, J. Karadamoglou, and X. Zotos, *Phys. Rev. B* **68**, 235106 (2003).